ADVANCED FUNCTIONAL MATERIALS
www.afm-journal.de

Materials Views
www.MaterialsViews.com

Giant Electrocaloric Response Over A Broad Temperature Range in Modified $BaTiO_3$ Ceramics

*Xiao-Shi Qian, Hui-Jian Ye, Ying-Tang Zhang, Haiming Gu, Xinyu Li, C. A. Randall, and Q. M. Zhang**

A giant electrocaloric effect (ECE) near room temperature is reported in a lead-free bulk inorganic material. By tuning $Ba(Zr_xTi_{1-x})O_3$ compositions which also exhibit relaxor ferroelectric response to near the invariant critical point, the $Ba(Zr_xTi_{1-x})O_3$ bulk ceramics at $x \sim 0.2$ exhibit a large adiabatic temperature drop of 4.5 K, a large isothermal entropy change of 8 J kg^{-1} K^{-1}, and a large EC coefficient ($|\Delta T_c/\Delta E| = 0.52 \times 10^{-6}$ KmV^{-1} and $\Delta S/\Delta E = 0.93 \times 10^{-6}$ J m kg^{-1} K^{-1} V^{-1}) over a 30 K temperature range. These properties added together indicate a general solution of the electrocaloric materials with high performance for practical cooling applications.

1. Introduction

Electrocaloric effect (ECE), an electric field induced temperature and/or entropy change of an insulating material, has attracted a great deal of attention after the recent findings of large ECE in ceramic thin films, polymers, and a dielectric fluid.[1–10] Several recent works have also demonstrated potential of realizing high performance cooling devices exploiting large ECE in new electrocaloric (EC) materials.[11–14] In these newly developed EC materials, the giant ECE, i.e., large adiabatic temperature change ΔT and isothermal entropy change ΔS, were obtained under high applied electrical fields. For example, a $|\Delta T| = 35$ K and $\Delta S = 160$ $Jkg^{-1}K^{-1}$ were induced in a high energy electron irradiated P(VDF-TrFE) relaxor polymer under an electric field change ΔE of 180 MVm^{-1}.[15] Analogously, in ferroelectric $BaTiO_3$ (BT) thick films, a $|\Delta T| = 7.1$ K and $\Delta S = 10.1$ $Jkg^{-1}K^{-1}$ were generated under the application of high electric fields change $\Delta E = 80$ MVm^{-1}.[16]

As one starts to address these EC materials for practical cooling devices applications, additional parameters should be considered besides a large ΔT and ΔS to measure the performance of EC materials. For instance, in order for cooling devices to be operated at low voltage such as <200 volts which is the normal voltage range for most cooling devices, an EC material with a large ECE induced under small electric fields is also important. In addition, a wide operational temperature range near room temperature is highly desired in order to develop high performance and practical EC cooling devices.[11–14] Therefore, one critical question is how to design and develop dielectric materials which are capable of generating giant ECE over a broad operation temperature with relatively low applied electric field change ΔE.

As a lead-free ferroelectric material which is environmentally friendly and is in fact the most widely used ferroelectric material, ECE in BT has been studied quite extensively in the past several years by many groups and in various forms including thin films, bulk ceramics (including thick films multilayer ceramic capacitors (MLCC)), and single crystals.[16–22] Large ΔT and ΔS have been reported in BT ceramics at temperatures near the ferroelectric-paraelectric (FE-PE) transition.[16] It is noted that for BT, besides the high temperature FE-PE transition (the transition temperature $T_{FE\text{-}PE} > 100$ °C) between the tetragonal ferroelectric (Tet) and cubic paraelectric phase, also exhibits an orthorhombic (O) and a rhombohedral (Rhom) phases as illustrated in **Figure 1**(a).[23] As ECE is directly related to the entropy change of an insulation dielectric under the change of the applied electric field, a dielectric with a polar phase which contains a large number of polar-states with similar energy levels can be induced under a reasonable electric field from a non-polar phase (i.e., below the dielectric breakdown field of the dielectric) has the potential of achieving giant ΔT and ΔS.[24,25] Moreover, a giant ECE can be induced under a low electric field ΔE if the energy barriers for switching between the polar-states are vanishingly small. For pure BT at the FE-PE transition, the FE tetragonal phase (Tet) has six equivalent polar-states and

X.-S. Qian, H. Gu, X. Li, Prof. Q. M. Zhang
Department of Electrical Engineering
and Materials Research Institute
The Pennsylvania State University
University Park, PA 16802, USA
E-mail: qxz1@psu.edu
Prof. Q. M. Zhang
Tsinghua University
Beijing, 100084, PR China
H.-J. Ye, Dr. Y.-T. Zhang, Prof. C. A. Randall
Materials Research Institute
The Pennsylvania State University
University Park, PA 16802, USA
H.-J. Ye
School of Materials Science and Engineering
Harbin Institute of Technology
Harbin, 150001, PR China
Dr. Y.-T. Zhang
School of Material Science and Engineering
Institute of Functional Material
Shaanxi University of Technology
Hanzhong, 723003, PR China
Prof. C. A. Randall
Department of Materials Science and Engineering
The Pennsylvania State University
University Park, PA 16802, USA

DOI: 10.1002/adfm.201302386

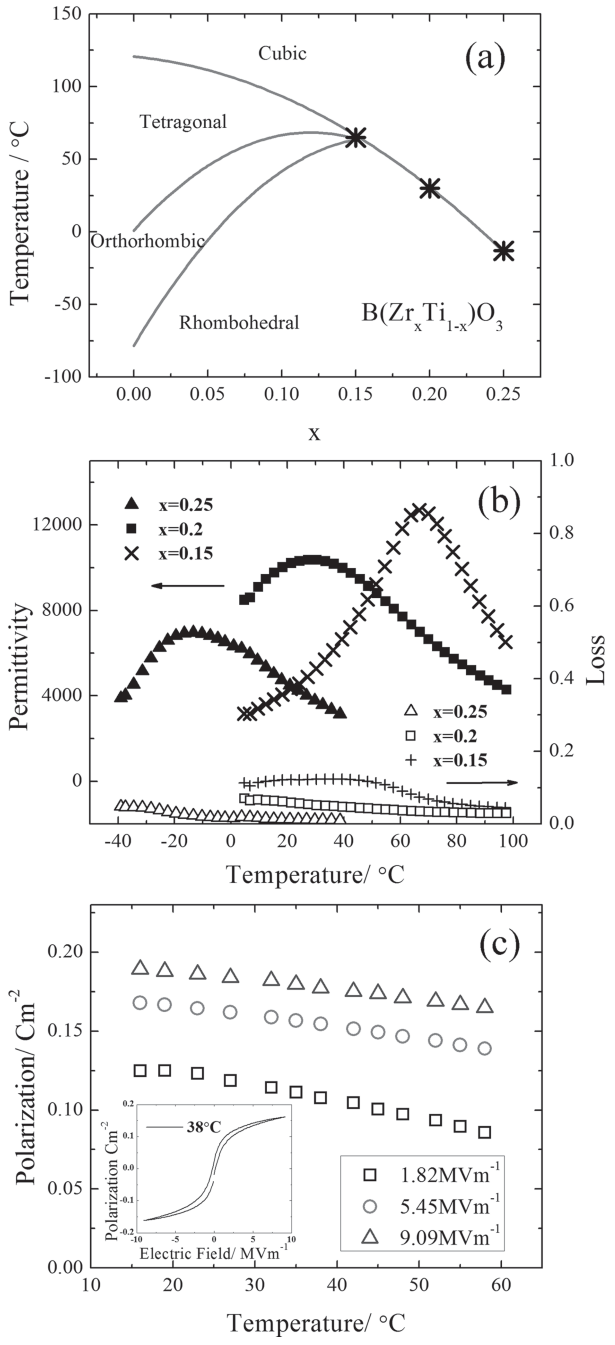

Figure 1. (a) Phase diagram of Ba(Zr$_x$Ti$_{1-x}$)O$_3$ solid solution systems.[23] Stars (*) are the dielectric constant maxima from this study. (b) Weak-field dielectric properties as functions of temperature for BZT(x = 0.15, 0.2 and 0.25). (c) Polarization as a function of temperature for BZT(x = 0.2) under different electric fields. The inset shows a polarization-electric field loop (P-E loop) for BZT(x = 0.2) at 38 °C.

a large dielectric constant at FE-PE transition causes a large ΔT/ΔE at temperatures right above the FE-PE transition, as has been observed in single crystal BT.[18] On the other hand, as suggested by Liu et al., by operating near an invariant critical point (ICP) at which all the four phases (paraelectric cubic, Tet, O, and Rhom) can coexist, their is an increased number of available polar states (twenty-six states) that leads to a significant increase in the entropy of the non-polar phase,[25] leading to giant ΔT and ΔS. Moreover, the near zero energy barriers near ICP imply a low field for inducing switching between these different states and hence a giant ECE can be induced under low electric fields.[25,26]

It is well known and has been extensively studied that the temperature of the three phase transitions in BT can be easily moved by chemical modifications in the BT.[23] As presented in Figure 1(a), by working with a solid solution of Ba(Zr$_x$Ti$_{1-x}$)O$_3$, these three transitions will merge into an ICP at x ~ 0.15, near which the four phases can coexist near room temperature.[23,27] Moreover, an early study has shown that BZT at compositions x > 0.2 exhibits ferroelectric relaxor response,[27] which can also enhance the ECE. In this paper, we demonstrate that indeed for BZT(x = 0.2), a relaxor composition near ICP occurs and a giant ECE property exists, i.e., both a large ΔT and ΔT/ΔE can be obtained near room temperature over a broad temperature range (from 25 to 50 °C) in bulk ceramic samples. The results presented here demonstrate a general approach to significantly enhance ECE in ferroelectrics with relatively low applied fields, which addresses a critical issue in applying these materials for practical cooling device applications.

2. Results and Discussions

In this study, BZT ceramics at compositions of x = 0.15, 0.2, and 0.25 were prepared and their ECE and related dielectric properties were characterized over the temperature range of interest (from 10 °C to 100 °C). The dielectric properties were characterized using an LCR meter (HP4284A) equipped with a temperature chamber (Delta9023).[28] Polarization-electric field (P-E) loops were measured using a Sawyer–Tower circuit.[34] A differential scanning calorimetry (DSC) (TA Q100) was used to characterize the thermal properties of the ceramics. The heat Q generated and absorbed as a result of ECE was directly measured using a specially designed calorimeter with a heat flux sensor (RdF P/N 27134–3).[7] In this set-up, when a constant voltage, V, with a pulse time duration, t (<0.5 seconds), is applied to a reference resistor heater R, a joule heat $Q_h = (V^2/R)t$ is produced. The heat generated is detected by a heat flux sensor that directly attached to the sample surface. Now, if the ECE sample under an applied electric field also generates (or absorbs) the same amount of heat as detected by the same heat flux sensor, then the heat Q_{ECE} from the ECE material is equal to Q_h. From $Q_h = Q_{ECE} = T\Delta S$, ΔS, an isothermal entropy change is determined. The adiabatic temperature change, ΔT, is deduced from $Q = \int_0^{\Delta T} c_E dT$ where c_E is the specific heat of the ceramic sample. As shown in Figure S1, the specific heat of these samples does not change significantly with temperature and in deducing ΔT, it was approximated that it is invariant also with the field. Figure S1 also shows that the specific heat of the three compositions does not differ significantly with temperatures ranging from 0 °C to 70 °C.

Figure 1(b) presents the dielectric properties measured at 1 kHz of BZT ceramics at x = 0.15, x = 0.2, and x = 0.25 compositions. The BZT(x = 0.2) samples display a broad dielectric

constant peak at 25 °C and relaxor dielectric response, consistent with earlier studies.[27] The induced polarization P vs. temperature, obtained from the polarization hysteresis loops taken from BZT(x = 0.2) sample at different applied field amplitudes at 100 Hz and temperatures, is presented in **Figure 2**(c). The induced polarization decreases with temperature continuously from 15 °C to 60 °C and does not exhibit any peak around 25 °C, consistent with the relaxor nature of the material. The dielectric peak of BZT(x = 0.15) occurs at a temperature near 67 °C and peak is narrower compared with that of BZT(x = 0.2). As shown in Figure S2, BZT at these compositions show slim polarization loops at temperatures near their respective dielectric peaks.

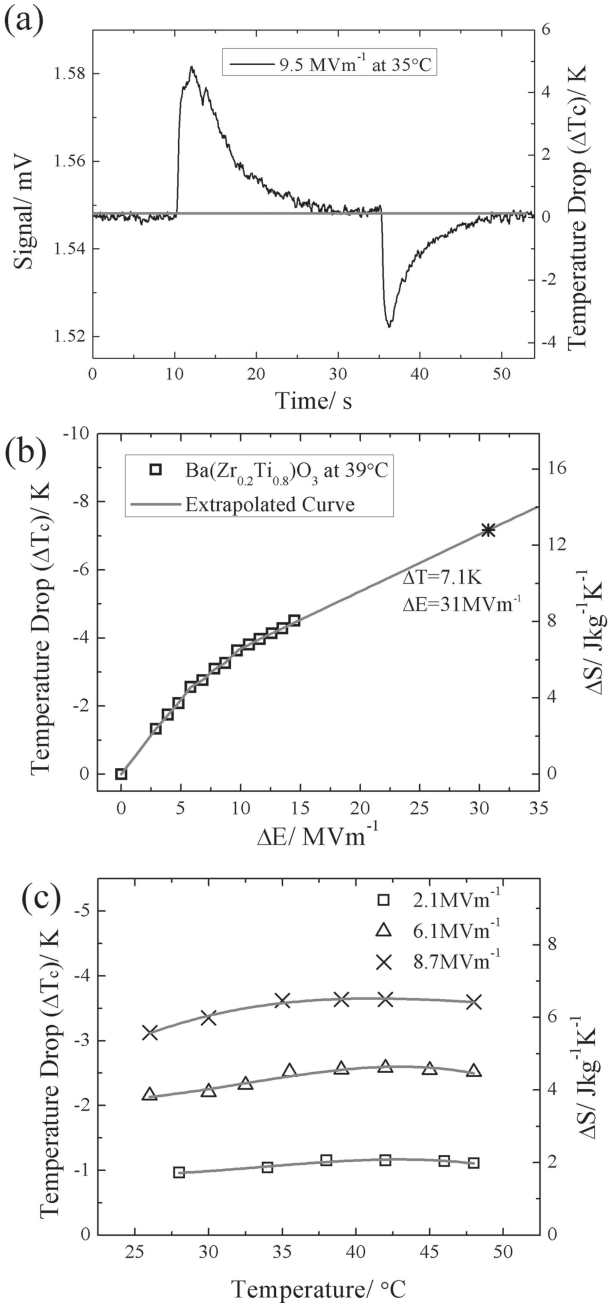

Figure 2. (a) The directly recorded ECE signal for BZT(x = 0.2) as the electric field was turning on and off, respectively. The data were measured under ΔE = 9.5 MVm^{-1} at 35 °C. Solid line is drawn to show the ambient temperature reading. (b) EC-induced temperature drop ΔT_c and isothermal temperature change ΔS as functions of ΔE for BZT(x = 0.2) at 39 °C. The data were extrapolated (solid curve) to estimate ΔT_c at higher electric fields. (c) ΔT_c and ΔS as functions of temperature for BZT(x = 0.2) under different electric fields. Solid curves are drawn to guide eyes.

ECE results of the three BZT compositions were characterized and BZT(x = 0.2) exhibits the highest EC response which also occurs near room temperature. BZT(x = 0.15) displays a slightly reduced ECE which peaks at 67 °C, compared with BZT(x = 0.2), but is higher than that of BZT(x = 0.25). Hence, detailed ECE studies were carried out for BZT(x = 0.15) and BZT(x = 0.2) which are presented in the paper.

The directly recorded ECE signal from BZT(x = 0.2) (at 35 °C under a ΔE = 9.5 MVm^{-1}) is presented in Figure 2(a), which shows the temperature rise and drop as the field is applied and removed from the ceramic sample. ΔS and ΔT_c from the temperature drop of the sample as the field is removed are presented in Figure 2(b) for the BZT(x = 0.2) at 35 °C under different ΔE. The data reveals that at ΔE = 14.5 MVm^{-1}, ΔT_c = – 4.5 K and ΔS = 8 $Jkg^{-1}K^{-1}$ (Q = 2.5 Jg^{-1}) are obtained. Here ΔT_c is introduced to represent the temperature drop (cooling) of the sample as the field is reduced. As shown in Figure 2(c), ΔT_c and ΔS do not show much change over a broad temperature range from 25 °C to 50 °C, and there is a very broad peak between 35 °C and 40 °C, higher than the broad dielectric constant peak temperature (= 25 °C). For the bulk BZT(x = 0.2) ceramic samples in the ECE study, the highest field that can be applied was 14.5 MVm^{-1}. To make a comparison with the results on BT thick films, we extrapolate the data in Figure 2(b) to higher fields and it is deduced that ΔT_c = –7.1 K can be induced for BZT(x = 0.2) ceramics under a field of 31 MVm^{-1}, which is more than two times lower than that required to induced the same ΔT_c (= 80 MVm^{-1}) in the pure BT ceramics. This extrapolation is consistent with the induced polarization data of this BZT composition (assuming ΔT_c is proportional to the square of the polarization P)[29] which can be measured up to 35 MVm^{-1}.The results are also consistent with prediction that giant ECE under low applied field can be achieved by operating near ICP to maximize the number of coexisting phases which have vanishing energy barriers to switch.[25,26]

To measure quantitatively how effective an applied electric field ΔE in generating ECE in dielectrics, the ratio of $\Delta T_c/\Delta E$, $\Delta S/\Delta E$ (or $Q/\Delta E$, where Q = TΔS) have been introduced in early studies.[18,30] In this paper, these parameters are referred to as the electrocaloric coefficients. Analogous to many materials coefficients of ferroelectric materials such as the piezoelectric coefficients which change with the measuring field amplitude ΔE,[10,30,31] the EC coefficients for BZT(x = 0.2) also change with ΔE. Large EC coefficients ($|\Delta T_c/\Delta E| = 0.52 \times 10^{-6}$ KmV^{-1} and $\Delta S/\Delta E = 0.93 \times 10^{-6}$ $Jmkg^{-1}K^{-1}V^{-1}$) are observed at ΔE = 2.1 MV/m and ΔT_c = –1.1 K. The coefficients decrease ($|\Delta T_c/\Delta E| = 0.31 \times 10^{-6}$ KmV^{-1} and $\Delta S/\Delta E = 0.54 \times 10^{-6}$ $Jmkg^{-1}K^{-1}V^{-1}$) at higher ΔE = 14.5 MVm^{-1} and ΔT_c = –4.5 K. In addition, the materials maintain the giant EC response over a broad temperature range, as indicated by Figure 2(c).

Figure 3(a) presents ΔT_c and ΔS of BZT(x = 0.15) measured at 69 °C vs. ΔE and the data were taken from the temperature

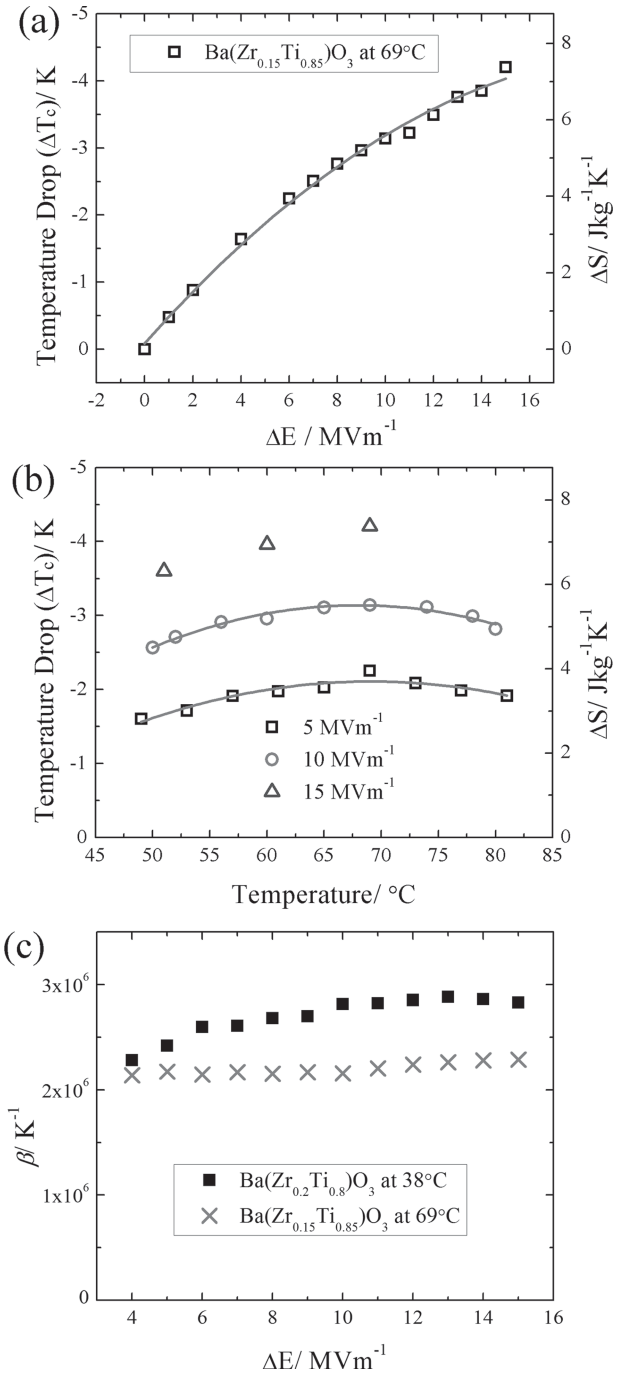

Figure 3. (a) Temperature drop as a function of applied field ΔE at 69 °C for BZT(x = 0.15). (b) Temperature drop ΔT_c and isothermal entropy change ΔS as functions of temperatures under different electric fields. (c) β coefficient as a function of electric fields for BZT(x = 0.15) and BZT(x = 0.2) near the temperature of their respective ECE peaks. Solid curves are drawn to guide eyes.

lowering of the sample as the field was removed. ΔT_c = –4.2 K and ΔS = 7.3 $Jkg^{-1}K^{-1}$ were induced under 15 MVm^{-1}. ΔT_c vs. temperature measured under different electric fields are shown in Figure 3(b) and a slightly larger temperature variation is observed, when compared with the data in Figure 2(c) for BZT(x = 0.2). ΔT_c shows a broad peak near 69°C. The EC coefficients $|\Delta T_c/\Delta E| = 0.48 \times 10^{-6}$ KmV^{-1} and $\Delta S/\Delta E = 0.85 \times 10^{-6}$ $Jmkg^{-1}K^{-1}V^{-1}$ for BZT(x = 0.15) under ΔE = 1 MVm^{-1}. The EC coefficients of BZT(x = 0.15) is slightly lower than that of BZT(x = 0.2). Similar to what is observed in BZT(x = 0.2), the EC coefficient is reduced to $|\Delta T_c/\Delta E| = 0.28 \times 10^{-6}$ KmV^{-1} and $\Delta S/\Delta E = 0.5 \times 10^{-6}$ $Jmkg^{-1}K^{-1}V^{-1}$ under a higher electric field ΔE = 15 MVm^{-1}. The study here as well as earlier studies all indicate that BZT(x = 0.15) is where the three transitions merge (ICP) while BZT(x = 0.2) exhibits "stronger" ferroelectric relaxor behavior compared with BZT(x = 0.15).[27] The results suggest that it is the combination of ICP and ferroelectric relaxor behavior that leads to the giant ΔT_c and $\Delta T_c/\Delta E$ in the ceramic BZT near room temperature.[7,25] This is also consistent with the β coefficient, where β is defined from, $\Delta S = -\frac{1}{2}\beta P^2$, from BZT with different compositions.[29] Figure 3(c) shows that β for BZT(x = 0.2) can be more than 25% higher than that of BZT(x = 0.15). On the other hand, further increasing the composition to x = 0.25 causes a reduction of ECE compared with that at x = 0.2.

Table 1 compares the ECE from this study with the EC materials such as ceramics and polymers that have potential for practical cooling applications. The ECE data from single crystals and thin films (such as sub-micron thick films supported on foreign substrates) are also included, which may not be directly used for practical cooling devices. It is worth mentioning that both ΔT and ΔS may also be derived from the pyroelectric coefficient $(\partial P/\partial T)$ of Figure 1(c) using the Maxwell relation (the pyroelectric coefficient data for both BZT(x = 0.15) and BZT(x = 0.2) was characterized).[1,2,29] It was found that the ΔT and ΔS thus derived (here the method is referred to as the indirect method) were very different from that directly measured, likely caused by the fact that these BZT compositions show relaxor ferroelectric behavior. An earlier experimental study from our group also showed that the indirect method may not necessarily yield reliable ECE data for relaxors.[28] Hence, the ECE results deduced from the indirect method are not included in Table 1. For practical applications, the temperature range in which a large ECE can be maintained is also critical.[11–14] In the Table, T_{span} is introduced to measure this performance, which is the temperature span over which the ΔT_c maintains 0.9 × ΔT_c(maximum). As can be seen, the BZT developed here possesses a giant ECE, i.e., large ΔT_c, $\Delta T_c/\Delta E$, $\Delta S/\Delta E$ and T_{span}. The combination of these high performances indicates the potential of the material developed here for the ECE based cooling devices with high cooling power and efficiency.

3. Conclusion

Our work demonstrates that ECE and EC coefficient can be greatly improved in lead-free bulk ceramics by modifying the BT ceramics to its ICP and turning it to relaxor ferroelectrics. BZT bulk ceramics are sintered and their EC responses are directly characterized. Large improvement of EC-induced temperature drop of 4.5 K and large EC coefficient around 0.5×10^{-6} KmV^{-1} are reported. Multi-phase coexistence near ICP provides more randomness in the system and hence more available polarization states. Moreover, the BT ceramics are tailored from ferroelectrics to relaxors after Zr is added to the system. The ceramic relaxor BZT(x = 0.2) shows a giant ECE

Table 1. Comparison of EC properties of BZTs developed here with those in the literature. ΔT_c is the temperature drop (cooling) in the ECE data. For the measurement methods, DSC refers to as the direct EC measurement using differential scanning calorimetry.

Material	Form	T [°C]	ΔT_c [K]	ΔE [MVm^{-1}]	$\lvert\Delta T_c/\Delta E\rvert$ [10^{-6}KmV^{-1}]	$\Delta S/\Delta E$ [10^{-6}Jmkg^{-1}K^{-1}V]	T_{span}. [K]	Method	Reference
BZT(x = 0.2) (high field)	Ceramic	39	4.5	14.5	0.31	0.54	>30	Direct	This work
BZT(x = 0.2) (low field)	Ceramic	38	1.1	2.1	0.52	0.93	>30	Direct	This work
BZT(x = 0.15)	Ceramic	69	4.2	15	0.28	0.5	>30	Direct	This work
BT	Ceramic	118	0.4	0.75	0.53		10	Direct	[17]
BT	Ceramic MLCC	80	7.1	80	0.09	0.12	80	DSC	[16]
BT	Ceramic MLCC	80	1.8	17.6	0.10			DSC	[8]
Doped BT	Ceramic MLCC	21	0.5	30	0.02	0.02	60	Direct	[32]
PMN	Ceramic	67	2.5	9	0.27			Direct	[10]
PMN-30PT	Ceramic	145	2.6	9	0.29			Direct	[10]
PLZT	Thin Film	45	40	120	0.33			Direct	[7]
Irradiated P(VDF-TrFE)	Polymer	33	35	180	0.13	0.63	50	Direct	[15]
P(VDF-TrFE-CFE)	Polymer	30	15.7	150	0.10	0.49	50	Direct	[33]
BT	Single Crystal	129	0.7	1.2	0.58	0.79	5	Direct	[18]
BT	Single Crystal	140	1.6	1	1.6	2.13	5	DSC	[19]
$Pb(Mg_{1/3}Nb_{2/3})_{0.75}Ti_{0.25}O_3$	Single Crystal	110	1.1	2.5	0.44			DSC	[5]

around room temperature and a wide EC operating temperature range which is promising in designing cooling devices.

4. Experimental Section

The BZT ceramic samples were fabricated by the conventional solid-state reaction methods. All the chemicals of barium carbonate ($BaCO_3$, 99.8%), zirconium dioxide (ZrO_2, 99.5%), and titanium dioxide (TiO_2, 99.5%) were purchased from Alfa Aesar and used without further purification. Stoichiometric weights of all the powder were milled by zirconia balls for 24 hours to obtain well-dispersed mixture. After the calcination at 1100 °C for 2 h, sintering of the pellets was performed at 1360 °C in air for 2 h with a heating rate of 3 °Cmin^{-1}. One wt% glass was added in before the sintering in order to improve the breakdown strength of the ceramics. The final ceramics after sintering were 10 mm in diameter and about 1 mm in thickness. A typical edge view of BZT(x = 0.2) is shown in Figure S3 taken by Scanning Electron Microscopy (FEI NanoSEM 630 FESEM). For electric characterization, the samples were polished to 100 µm thick. Au electrodes were sputtered on the sample surfaces for the electric characterizations.

Supporting Information

Supporting Information is available from the Wiley online Library or from the author.

Acknowledgements

This work was supported by Army Research Office under grant W911NF-11–1–0534. Hui-jian Ye and Dr. Ying-tang Zhang were also in part supported by Chinese Scholarship Council.

Received: July 16, 2013
Published online: September 13, 2013

[1] A. S. Mischenko, Q. Zhang, J. F. Scott, R. W. Whatmore, N. D. Mathur, *Science* **2006**, *311*, 1270.
[2] B. Neese, B. J. Chu, S. G. Lu, Y. Wang, E. Furman, Q. M. Zhang, *Science* **2008**, *321*, 821.
[3] X. S. Qian, S. G. Lu, X. Li, H. Gu, L. C. Chien, Q. M. Zhang, *Adv. Func. Mater.* **2013**, *23*, 2894.
[4] A. S. Mischenko, Q. Zhang, R. W. Whatmore, J. F. Scott, N. D. Mathur, *Appl. Phys. Lett.* **2006**, *89*, 242912.
[5] G. Sebald, L. Seveyrat, D. Guyomar, L. Lebrun, B. Guiffard, S. Pruvost, *J. Appl. Phys.* **2006**, *100*, 124112.
[6] B. Neese, S. G. Lu, B. Chu, Q. M. Zhang, *Appl. Phys. Lett.* **2009**, *94*, 042910.
[7] S. G. Lu, B. Rožič, Q. M. Zhang, Z. Kutnjak, X. Li, E. Furman, L. J. Gorny, M. Lin, B. Malič, M. Kosec, R. Blinc, R. Pirc, *Appl. Phys. Lett.* **2010**, *97*, 162904.
[8] Y. Bai, G. Zheng, S. Shi, *Appl. Phys. Lett.* **2010**, *96*, 192902.
[9] F. Le Goupil, A. Berenov, A.-K. Axelsson, M. Valant, N. M. Alford, *J. Appl. Phys.* **2012**, *111*, 124109.
[10] B. Rožič, M. Kosec, H. Uršič, J. Holc, B. Malič, Q. M. Zhang, R. Blinc, R. Pirc, Z. Kutnjak, *J. Appl. Phys.* **2011**, *110*, 064118.
[11] H. Gu, B. Craven, X. S. Qian, X. Li, A. Cheng, Q. M. Zhang, *Appl. Phys. Lett.* **2013**, *102*, 112901.
[12] H. Gu, X. S. Qian, X. Li, B. Craven, W. Zhu, A. Cheng, S. C. Yao, Q. M. Zhang, *Appl. Phys. Lett.* **2013**, *102*, 122904.
[13] Y. S. Ju, *J. Electron. Packag.* **2010**, *132*, 041004.
[14] Y. Jia, Y. S. Ju, *Appl. Phys. Lett.* **2012**, *100*, 242901.
[15] X. Li, X. S. Qian, H. Gu, X. Z. Chen, S. G. Lu, M. Lin, F. Bateman, Q. M. Zhang, *Appl. Phys. Lett.* **2012**, *101*, 132903.
[16] Y. Bai, G.-P. Zheng, K. Ding, L. Qiao, S.-Q. Shi, D. Guo. *J. Appl. Phys.* **2011**, *110*, 094103.
[17] A. I. Karchevskii, *Sov. Phys. – Solid State.* **1962**, *3*, 2249.
[18] X. Moya, E. Stern-Taulats, S. Crossley, D. González-Alonso, S. Kar-Narayan, A. Planes, L. Mañosa, N. D. Mathur, *Adv. Mater.* **2013**, *25*, 1360.
[19] Y. Bai, K. Ding, G.-P. Zheng, S.-Q. Shi, L. Qiao, *Phys. Status Solidi A* **2012**, *209*, 941.
[20] G. Akcay, S. P. Alpay, J. V. Mantese, G. A. Rossetti Jr., *Appl. Phys. Lett.* **2007**, *90*, 252909.

[21] X. Zhang, J. B. Wang, B. Li, X. L. Zhong, X. J. Lou, Y. C. Zhou, *J. Appl. Phys.* **2011**, *109*, 126102.
[22] S. P. Beckman, L. F. Wana, J. A. Barra, T. Nishimatsua, *Mater. Lett.* **2012**, *89*, 254.
[23] B. Jaffe, W. R. Cook Jr., H. Jaffe, *Piezoelectric Ceramics*, Academic Press Limited, OH, USA **1971**.
[24] R. Pirc, Z. Kutnjak, R. Blinc, Q. M. Zhang. *Appl. Phys. Lett.*, **2011**, *98*, 021909.
[25] Z. K. Liu, Xinyu Li, Q. M. Zhang, *Appl. Phys. Lett.* **2012**, *101*, 082904.
[26] Z. Kutnjak, J. Petzelt, R. Blinc, *Nature* **2006**, *441*, 956.
[27] Z. Yu, R. Guo, A. S. Bhalla, *J. Appl. Phys.* **2000**, *88*, 410.
[28] S. G. Lu, B. Rožič, Q. M. Zhang, Z. Kutnjak, R. Pirc, M. Lin, X. Li, L. Gorny, *Appl. Phys. Lett.* **2010**, *97*, 202901.
[29] S. G. Lu, Q. M. Zhang, *Adv. Mater.* **2009**, *21*, 1983.
[30] N. Novak, R. Pirc, Z. Kutnjak, *Phys. Rev. B* **2013**, *87*, 104102.
[31] V. Mueller, Q. M. Zhang, *J. Appl. Phys.* **1998**, *72*, 2692.
[32] S. Kar-Narayan, N. D. Mathur *J. Phys. D: Appl. Phys.* **2010**, *43*, 032002.
[33] X. Li, X. S. Qian, S. G. Lu, J. Cheng, Z. Fang, Q. M. Zhang, *Appl. Phys. Lett.* **2011**, *99*, 052907.
[34] S. Wu, W. Li, M. Lin, Q. Burlingame, Q. Chen, A. Payzant, K. Xiao, Q. M. Zhang, *Adv. Mater.* **2013**, *25*, 1734.